

Lattice superstring and noncommutative geometry

J. Nishimura^a

^a High Energy Accelerator Research Organization (KEK)

1-1 Oho, Tsukuba 305-0801, Japan

Recent developments in superstring theory and noncommutative geometry are deeply related to the idea of Eguchi-Kawai reduction in large N gauge theories which dates back to early 80s. After a general review on this subject including revived interests in solving planar QCD, we present some results in the superstring matrix model suggesting the dynamical generation of 4d space-time due to the collapse of the eigenvalue distribution. We then discuss interesting dynamical properties of field theories in noncommutative geometry, which have been revealed by Monte Carlo simulations of twisted reduced models. We conclude with a comment on the recent proposal for a lattice construction of supersymmetric gauge theories based on reduced models.

1. Introduction

Superstring theory is a unified theory where matter and gauge particles are both described by various oscillation modes, while all the interactions including gravity are described simply by joining and splitting of strings. Unification of interactions is not only motivated for aesthetic reasons but also suggested by precise measurements of the coupling constants in the Standard Model.

In fact superstring theory is so far the only quantum theory of gravity that is perturbatively well-defined preserving manifest unitarity. This is in sharp contrast to the situation with the field theoretical approach treating the metric as a quantum field, where the theory is perturbatively unrenormalizable. Here one has to study a regularized theory nonperturbatively and hope to find a nontrivial UV fixed point, where one can take the continuum limit. This has been a topic studied over a decade. There is still a possibility that a sensible continuum limit can be taken, but the issue of unitarity remains unclear.

The problem with superstring theory, on the other hand, is that there are too many perturbatively stable vacua with various space-time dimensionality, gauge group, matter contents and so on. This means that non-perturbative effects are crucial for understanding the ‘true vacuum’, which hopefully describes our world.

At this point let us recall the history of QCD. Properties of its vacuum such as confinement and chiral symmetry breaking as well as the dynamics of low energy excitations have been understood by a nonperturbative formulation of gauge theory, namely the lattice gauge theory. Likewise matrix models, which provide a nonperturbative formulation of string theory, are expected to give new insights into the nonperturbative dynamics of string theory.

The particular type of matrix models we will be discussing appeared in history as large N reduced models in the context of solving $SU(\infty)$ gauge theory [1]. The matrix model proposed as a non-perturbative formulation of superstring theory in ten dimensions [2] can be regarded as one of such models. Among various dynamical issues, we will focus on an exciting possibility, which has been discussed by many authors [3,4,5,6,7,8,9,10,11,12,13,14], that the $SO(10)$ symmetry of the model is spontaneously broken down to $SO(4)$ and the 4d space-time appears *dynamically*.

String theory has deep connections to noncommutative geometry, and large N reduced models naturally incorporate this feature [15,16]. In fact a certain type of reduced models [17] provides a lattice regularization of field theories on noncommutative geometry [18,19,20]. We will review some Monte Carlo results [21,22,23], which reveal interesting nonperturbative dynamics of such the-

ories.

The reduced model describing nonperturbative superstrings has manifest supersymmetry even for finite N and this feature has been utilized recently for a lattice formulation of supersymmetric gauge theories [24]. There are also revived interests in solving $SU(\infty)$ gauge theories with new ideas for treating massless fermions and topologies of the gauge field [25,26]. In this review we also cover these new topics clarifying their mutual relationship.

This article is organized as follows. In Section 2 we discuss the connection between matrix models and string theory. In Section 3 we introduce the large N reduced models and discuss their equivalence to $SU(\infty)$ gauge theories. We also review some recent proposals in this direction. In Section 4 we describe the large N reduced model proposed as a nonperturbative formulation of superstring theory and discuss in particular the dynamical generation of 4d space-time. In Section 5 we discuss the connection between large N reduced models and noncommutative geometry. We present Monte Carlo results for Yang-Mills theory and ϕ^4 theory on noncommutative spaces, and discuss their intriguing dynamical properties. In Section 6 we comment on the relation to the recent proposal for a lattice formulation of supersymmetric gauge theories. Section 7 is devoted to a summary and conclusions.

2. How matrix models describe strings

In this Section we review briefly how matrix models are related to string theory. For illustration let us consider a simple matrix model defined by the action

$$S_{\text{mat}} = \frac{1}{2} N \text{tr} \phi^2 - \frac{1}{3} N \lambda \text{tr} \phi^3, \quad (1)$$

where ϕ is a $N \times N$ Hermitian matrix. This model can be solved exactly in the large N limit [27], but in order to see the connection to string theory, we make an expansion with respect to the cubic coupling constant λ . Since the dynamical variable ϕ has two indices, we use the double-line notation, which is convenient in discussing the large N limit.

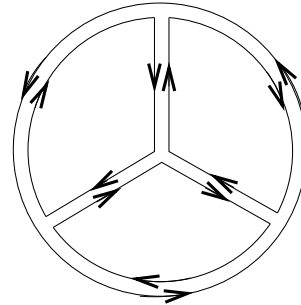


Figure 1. A 3-loop vacuum diagram which appears in the perturbative expansion of the ϕ^3 matrix model.

A typical vacuum diagram which appears as a $O(\lambda^4)$ contribution to the free energy is shown in Fig. 1. Each propagator carries $1/N$ and each vertex carries $N\lambda$, according to the Feynman rule, which can be read off from the action (1). A general vacuum diagram \mathcal{D} with V vertices, P propagators and I index loops can therefore be evaluated as

$$\mathcal{D} \sim \left(\frac{1}{N}\right)^P (N\lambda)^V N^I = \lambda^V N^\chi. \quad (2)$$

An important point here is that the power of N is given by the Euler number $\chi = V - P + I = 2(1 - h)$, which is given by the ‘genus’ h , namely the number of handles of the two-dimensional closed orientable surface, on which the diagram can be drawn without crossings of lines. For the diagram in Fig. 1 we have $V = 4$, $P = 6$, $I = 4$, hence $h = 0$. (Such diagrams are called ‘planar diagrams’ since they can be drawn on a plane without crossings of lines as in Fig. 1.)

As one can see from (2), if one takes the large N limit for fixed λ , only planar diagrams ($h = 0$) survive. Considering the Feynman diagrams as discretized two-dimensional surface, the continuum limit should be taken along with the fine-tuning of λ ensuring that contributions from higher orders in λ become dominant. This is known to be possible by sending λ to the critical value λ_c given by $(\lambda_c)^2 = \frac{1}{12\sqrt{3}}$ [27]. This

way of taking the limits (first $N \rightarrow \infty$ and then $\lambda \nearrow \lambda_c$) is relevant to 2d quantum gravity with fixed (spherical) topology, if one regards the 2d surface as the space-time. If instead one regards the 2d surface as the ‘worldsheet’ describing the time-evolution of strings, one may view this theory as a classical (or tree-level) string theory, since there is no branching.

In this regard let us note that the genus h gives the number of loops in the corresponding diagram in string theory. In order to obtain all the loop diagrams in string theory, one has to make diagrams with any genus survive the large N limit. In the present model this is achieved by the so-called double scaling limit, which is to take the $N \rightarrow \infty$ limit and the $\lambda \nearrow \lambda_c$ limit simultaneously keeping $N^2|\lambda - \lambda_c|^{5/2}$ fixed [28,29,30]. This provides a nonperturbative formulation of bosonic (non-critical) string theory. In this way one may regard matrix models as ‘lattice string theory’.

3. Large N reduced models

The connection between matrix models and string theory that we reviewed in the previous Section is quite general. But from now on we will focus on a particular class of matrix models which is known as large N reduced models. Historically they appeared in the context of solving $SU(\infty)$ gauge theory.

3.1. Eguchi-Kawai equivalence

Let us consider $SU(N)$ lattice gauge theory¹ on a L^D lattice (D -dimensional hypercubic lattice with the linear extent L) with the periodic boundary conditions. Then in the large N (planar) limit, Eguchi and Kawai [1] suggested that the model with $L = \infty$ is equivalent to the model with $L = 1$, namely the one-site model defined by the action

$$S_{\text{EK}} = -N\beta \sum_{\mu \neq \nu} \text{tr} (U_\mu U_\nu U_\mu^\dagger U_\nu^\dagger) . \quad (3)$$

¹In this article we will be sloppy about $SU(N)$ or $U(N)$ to simplify the description since they become equivalent in the large N limit. For instance, the U_μ in (3) should be *special*-unitary, and the symmetry (4) should be $(Z_N)^D$ if we really start from $SU(N)$ lattice gauge theory.

The dynamical variables in this Eguchi-Kawai model are given by D unitary matrices of size N . (This implies a huge reduction of dynamical degrees of freedom in the large N limit as indicated in the title of Ref. [1].)

In the proof of this statement, there was an important assumption that the $U(1)^D$ symmetry

$$U_\mu \mapsto e^{i\alpha_\mu} U_\mu \quad (4)$$

of the model (3) is not spontaneously broken. However it was soon noticed by Bhanot, Heller and Neuberger [31] that the $U(1)^D$ symmetry is actually broken at large β (weak coupling) for $D > 2$. This was shown by considering the eigenvalue distribution of the unitary matrix U_μ . At $\beta < \beta_c$ the eigenvalues lie uniformly on the unit circle, but at $\beta > \beta_c$ the eigenvalues are concentrated around some point on the unit circle. Since the $U(1)^D$ transformation (4) amounts to rotating all the eigenvalues around the unit circle, any non-uniform eigenvalue distribution signals the SSB. This does not occur at $D = 2$ in accord with the Mermin-Wagner theorem.

3.2. Remedies to the original proposal

After the discovery of the $U(1)^D$ SSB, remedies to the original proposal have been suggested. The authors of Ref. [31] proposed the quenched Eguchi-Kawai model. Their idea was to constrain the eigenvalues of U_μ to be uniformly distributed on the unit circle. This can be achieved by inserting

$$\int dV_\mu \delta(U_\mu - V_\mu Q V_\mu^\dagger) \quad (5)$$

in the partition function, where Q is a diagonal unitary matrix $Q = \text{diag}(1, \omega, \omega^2, \dots, \omega^{N-1})$ with $\omega = \exp(2\pi i/N)$.

Another proposal was made by Gonzalez-Arroyo and Okawa [17]. Their idea was to consider a L^D lattice with *twisted* boundary conditions, instead of the periodic ones, and then set $L = 1$. The one-site model thus obtained has the action

$$S_{\text{TEK}} = -N\beta \sum_{\mu \neq \nu} Z_{\mu\nu} \text{tr} (U_\mu U_\nu U_\mu^\dagger U_\nu^\dagger) , \quad (6)$$

where the Z_N factor $Z_{\mu\nu}$ comes from the twist in the boundary conditions. This model is called

the twisted Eguchi-Kawai model. Modifying the boundary conditions does not alter the thermodynamic limit $L = \infty$, but it does change the property of the $L = 1$ model drastically. The configurations which minimize the action are now given by $U_\mu^{(0)}$ which satisfies

$$U_\mu^{(0)} U_\nu^{(0)} = Z_{\mu\nu}^* U_\nu^{(0)} U_\mu^{(0)} . \quad (7)$$

The solution to this equation is unique up to the symmetry of the algebra for appropriate choice of the twist. Most importantly the minimum-action configuration $U_\mu^{(0)}$ has a uniform eigenvalue distribution, which prevents the SSB of $U(1)^D$ at large β . The Eguchi-Kawai equivalence of the twisted reduced models is reexamined in Ref. [32].

Recently Narayanan and Neuberger [26] proposed to consider a partially reduced model with $L > 1$ without quenching or twisting. The key observation is that the Eguchi-Kawai equivalence holds for arbitrary L as far as $U(1)^D$ is not spontaneously broken. The critical $\beta = \beta_c(L)$ at which the SSB occurs depends on L , and in particular $\beta_c(L) \rightarrow \infty$ as $L \rightarrow \infty$. Therefore one can always choose L such that the β one wants to study lies below the critical point $\beta_c(L)$.

Various extensions of the Eguchi-Kawai model were considered in the 80s. Matter fields in the adjoint and fundamental representations have been implemented in Refs. [33,34,35]. Extensions to non-gauge theories [36,37,38] and to finite temperature [39,40] are also studied intensively. For a comprehensive review on these subjects, we refer the reader to Ref. [41].

3.3. Revived interests in planar QCD

In Ref. [25] Kiskis, Narayanan and Neuberger proposed to study planar QCD along the idea of Eguchi-Kawai reduction. The underlying assumption is of course that QCD ($N_c = 3$) is actually not far from $N_c = \infty$ as evidenced in the glueball mass spectrum. Then the motivation for going to the limit $N_c = \infty$ comes from the fact that the valence quark approximation² becomes exact as far as the number of flavors N_f is kept finite. Hence all the pathologies observed with

²This is usually called ‘the quenched approximation’, but we prefer not to use this word to avoid confusion with the quenching in the reduced model.

this approximation at $N_c = 3$ should go away in the $N_c \rightarrow \infty$ limit, and one can make better sense out of Monte Carlo data without having to include the dynamical fermions. This is very attractive given that the full QCD simulation is still costly.

The reason for the exactness of the valence quark approximation in the large N_c limit can be readily seen by comparing the fermion loop and the gluon loop. In the double-line notation the color index loop running along the gluon loop is replaced by the flavor index loop in the case of the fermion loop because the fermion is in the fundamental representation with respect to the color $SU(N_c)$. This means that the fermion loop is suppressed by $O(N_f/N_c)$ compared with the gluon loop.

If one takes also the $N_f \rightarrow \infty$ limit together with the $N_c \rightarrow \infty$ limit with fixed $r \equiv N_f/N_c$, which is referred to as the Veneziano limit, the effects of sea quarks survive. By varying the parameter r , one can smoothly interpolate between the valence QCD and the full QCD.

For the present purpose, one should use the quenched Eguchi-Kawai model [31] or the partially reduced model [26] because the twisted Eguchi-Kawai model allows only integer r [35]. The authors of Ref. [25] also suggest to use the overlap Dirac operator [42], which enables the inclusion of exactly massless fermions in the model. The problem with the definition for the topological charge mentioned at the end of Section 3.4 is also solved by considering the overlap Dirac operator. Correct chiral anomalies have been reproduced from the reduced models in Refs. [43,44].

3.4. Continuum version of reduced models

Before concluding this Section we comment on the ‘continuum version’ of large N reduced models, which is important because manifest supersymmetry is implementable. The matrix model describing superstrings in ten dimensions falls into this category. This version has also been used in a lattice construction of supersymmetric gauge theories.

Let us recall that the Eguchi-Kawai model has been obtained by considering $SU(N)$ lattice gauge theory and setting the lattice size to $L = 1$. Sim-

ilarly let us start with continuum $SU(N)$ gauge theory and take the zero-volume limit. The reduced model one obtains in this way is given by the action

$$S_b = -\frac{1}{4g^2} \text{tr} [A_\mu, A_\nu]^2, \quad (8)$$

where A_μ ($\mu = 1, \dots, D$) are $N \times N$ Hermitian matrices.

This model has been studied intensively as the bosonic version of the superstring matrix model. The finiteness of the partition function (for $D > 2$ and sufficiently large N), which is nontrivial because the integration region of Hermitian matrices is non-compact, was shown first numerically [45,46] and proved later [47] (see Ref. [48] for a recent analytic work on observables). Ref. [49] studies the large N behavior of various correlation functions and in particular the $SO(D)$ symmetry is shown to be unbroken. This means that the dynamical generation of space-time expected in the $D = 10$ supersymmetric model does not occur in the bosonic version.

In spite of the importance of such Hermitian matrix models in the context of superstrings and supersymmetric gauge theories, their equivalence to large N gauge theory is dubious. Ref. [50] studies the VEV of the Wilson loop numerically in the $D = 4$ bosonic case. The area law holds in a finite regime, but this regime neither extends nor shrinks in the large N limit. The situation in the supersymmetric case is expected to be better [51], but the achieved N ($N = 48$) is not as large as in the bosonic case ($N = 768$).

The failure of Eguchi-Kawai equivalence in the Hermitian matrix models may be attributed to the breaking of the $U(1)^D$ symmetry, which now reads

$$A_\mu \mapsto A_\mu + \alpha_\mu \mathbf{1}. \quad (9)$$

As in the lattice version, one may consider twisting or quenching to remedy the situation. It is known that twisting is possible only formally at $N = \infty$ [52]. Quenching, on the other hand, seems to work at least perturbatively, but the naive definition of the topological charge $Q = \text{tr} F_{\mu\nu} \tilde{F}_{\mu\nu}$ vanishes identically [33].

4. Lattice superstring

4.1. The IKKT model

In 1996 Ishibashi, Kawai, Kitazawa and Tsuchiya conjectured that a simple reduced model provides a nonperturbative definition of type IIB superstring theory in ten dimensions [2]. The model, which is now referred to as the IIB matrix model or the IKKT model, can be obtained by taking the zero-volume limit of 10-dimensional $SU(N)$ super Yang-Mills theory in the continuum. The action is given explicitly as

$$S_{\text{IKKT}} = S_b + S_f, \quad (10)$$

$$S_f = -\frac{1}{2g^2} (\Gamma_\mu)_{\alpha\beta} \text{tr} (\Psi_\alpha [A_\mu, \Psi_\beta]), \quad (11)$$

where S_b is the bosonic part (8) and Ψ_α ($\alpha = 1, \dots, 16$) are $N \times N$ Hermitian fermionic matrices, which transform as Majorana-Weyl fermions under $SO(10)$ transformation. The 16×16 matrices Γ_μ are Weyl-projected γ -matrices in the Majorana representation.

There are by now a number of evidences for this conjecture. We list some of the most crucial ones. Firstly the action (10) can be regarded as a matrix regularization of the worldsheet action of the type IIB superstring theory. Secondly there are solitonic objects in string theory, which are known as ‘D-branes’, and the IKKT model contains these objects as classical solutions. Moreover the interaction between D-branes calculated in the matrix model agrees with the calculations in string theory. This is remarkable since the interaction includes gravity. Thirdly there is an attempt to derive the string field Hamiltonian from Schwinger-Dyson equations in the matrix model [53,54]. The derivation is successful albeit with the aid of a crude power-counting argument. This connection, if completed, would provide a direct proof of the conjecture.

There are various dynamical issues that should be addressed in this model. Some of them have been studied in simplified versions [49,51,55,56]. Here we will focus on the possibility that 4d space-time appears dynamically in the IKKT model.

4.2. Emergence of 4d space-time

Let us first discuss how the space-time is described in this model [3]. For that we diagonalize the matrix A_μ as

$$A_\mu = V_\mu X_\mu V_\mu^\dagger, \quad (12)$$

where X_μ is a real diagonal matrix $X_\mu = \text{diag}(x_{1\mu}, x_{2\mu}, \dots, x_{N\mu})$. By integrating out the unitary matrices V_μ first, one obtains diagrams like Fig. 1, but now each index loop is associated with $\vec{x}_i = (x_{i1}, x_{i2}, \dots, x_{i10})$, which may be viewed as describing the embedding of the world-sheet into the 10-dimensional target space. Thus we find that the eigenvalues of A_μ represent the space-time coordinates. This means in particular that the space-time is treated dynamically in this model. If the eigenvalue distribution of A_μ collapses to a 4d hypersurface in the 10d space-time, we are going to obtain 4d space-time *dynamically* in this model. This requires the $\text{SO}(10)$ symmetry of the model to be spontaneously broken.

The order parameter for the SSB can be defined as follows. Let us define the ‘moment of inertia tensor’ of the space-time as

$$T_{\mu\nu} = \frac{1}{N} \text{tr}(A_\mu A_\nu). \quad (13)$$

This matrix has 10 real positive eigenvalues, which we denote as λ_i ($i = 1, \dots, 10$) with the fixed ordering

$$\lambda_1 \geq \lambda_2 \geq \dots \geq \lambda_{10}. \quad (14)$$

If the ratio $\frac{\langle \lambda_1 \rangle}{\langle \lambda_{10} \rangle}$ does not approach unity in the $N \rightarrow \infty$ limit, it signals the SSB. More specifically, if $\langle \lambda_i \rangle$ with $i = 1, \dots, 4$ turn out to be much larger than $\langle \lambda_i \rangle$ with $i = 5, \dots, 10$, it implies the dynamical generation of 4d space-time.

4.2.1. Gaussian expansion method

In Refs.[10,11,12] this issue has been addressed by the Gaussian expansion method. In general the method amounts to considering the action

$$S_{\text{GEM}} = \frac{1}{\xi} (S_0 + S - \xi S_0), \quad (15)$$

where S is the action of the model one wants to study, and S_0 is a Gaussian action. If one sets $\xi = 1$ one retrieves the original action S . Then

one calculates various quantities as an expansion with respect to ξ up to some finite order and set $\xi = 1$. This yields a loop expansion considering $(S_0 + S)$ as the ‘classical action’ and $-S_0$ as the ‘one-loop counter-term’. The freedom in choosing the Gaussian action S_0 is crucial in this method.

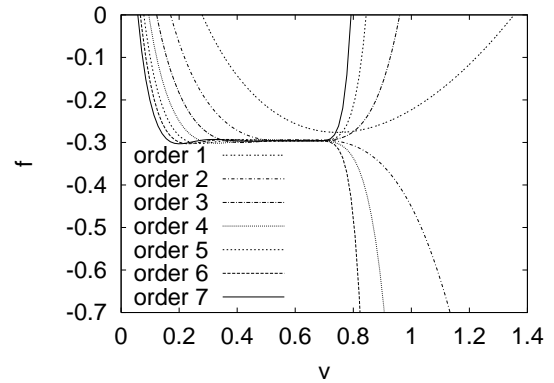


Figure 2. The free energy of the bosonic model obtained by the Gaussian expansion method is plotted as a function of v for $D = 10$. Each curve corresponds to the order 1, 2, \dots , 7.

Let us first describe how the method works in the bosonic version (8) of the IKKT model [57], where Monte Carlo results [49] are available. Since we know that the $\text{SO}(D)$ symmetry is not spontaneously broken in this model [49], we take the Gaussian action to be

$$S_0 = \frac{N}{v} \text{tr}(A_\mu)^2 \quad (16)$$

for simplicity,³ where the parameter v is left arbitrary at this point.

In Fig. 2 we plot the free energy obtained in the Gaussian expansion at various orders as a function of the parameter v in (16). Since v is a parameter which is introduced by hand, the result

³One may also consider $\text{SO}(D)$ breaking Gaussian action such as $S_0 = \sum_\mu \frac{N}{v_\mu} \text{tr}(A_\mu)^2$. The method works as well, and reproduces correctly the absence of SSB in the bosonic model.

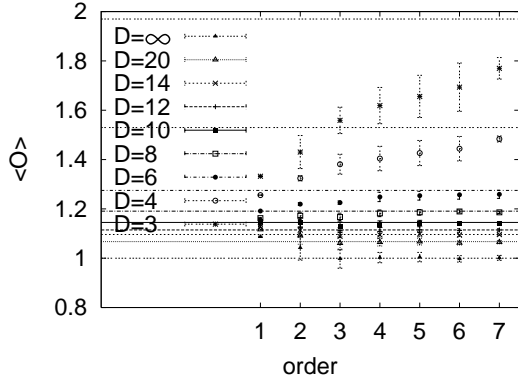


Figure 3. The observable $\langle \frac{1}{N} \text{tr}(A_\mu)^2 \rangle$ in the bosonic model obtained by the Gaussian expansion method at orders 1, \dots , 7 for various D . The horizontal lines represent either the Monte Carlo results ($D < \infty$) or the exact result ($D = \infty$).

should not depend much on it if the expansion becomes valid for some value of v . Remarkably we do see a clear plateau in Fig. 2, and the height of the plateau stabilizes with the increasing order. Similar behaviors were obtained for the observable $\langle \frac{1}{N} \text{tr}(A_\mu)^2 \rangle$, and the height of the plateau estimated at each order (with the ‘error bar’ representing the uncertainty) is shown in Fig. 3. The results converge to the horizontal lines, which represent either the Monte Carlo results ($D < \infty$) or the exact result ($D = \infty$). The convergence becomes faster for larger D .

Let us turn to the IKKT model (10), and describe how the first evidence for the 4d space-time was obtained in Ref. [10]. Since the SSB of the $\text{SO}(10)$ symmetry is the main issue here, the Gaussian action

$$S_0 = \sum_{\mu} \frac{N}{v_{\mu}} \text{tr}(A_{\mu})^2 + \sum_{\alpha\beta} N \mathcal{A}_{\alpha\beta} \text{tr}(\Psi_{\alpha} \Psi_{\beta}), \quad (17)$$

which breaks the $\text{SO}(10)$ invariance, was considered, and the Gaussian expansion has been performed up to the 3rd order. Since it is difficult to search for plateaus in the whole space of v_{μ} and $\mathcal{A}_{\alpha\beta}$, it was assumed that $\text{SO}(d)$ times some dis-

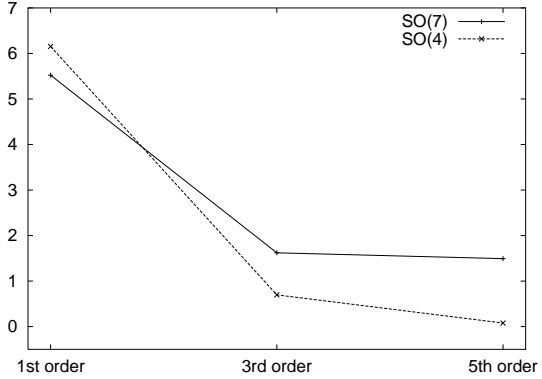


Figure 4. The free energy obtained by the Gaussian expansion method for the IKKT model at orders 1, 3 and 5. The two symbols correspond to the $\text{SO}(4)$ Ansatz and the $\text{SO}(7)$ Ansatz respectively. At the 3rd order and higher the free energy for the $\text{SO}(4)$ Ansatz becomes lower than the other.

crete subgroup of $\text{SO}(10-d)$, where $d = 2, 4, 6, 7$, is preserved. This assumption reduced the number of parameters to three, and plateaus were searched for by finding extrema of the free energy with respect to the three parameters for each d . At order 3, it was found that the solution for $d = 4$ gives the smallest free energy. The extent of the space-time in the d dimensions (R) and that in the remaining $(10-d)$ dimensions (r) have been estimated at the points in the parameter space which extremize the free energy. The ratio R/r turned out to be larger than one, and for $d = 4$ it increased drastically as one goes from order 1 to order 3.

A lot of effort has been made to increase the order of the expansion. It was soon noticed that Schwinger-Dyson equations can be used to reduce the number of Feynman diagrams to be evaluated [11]. Then a computer code has been written in order to automatize the task of listing up and evaluating all the Feynman diagrams [12]. With these technical developments, the order of the expansion has now been increased up to the 7th or-

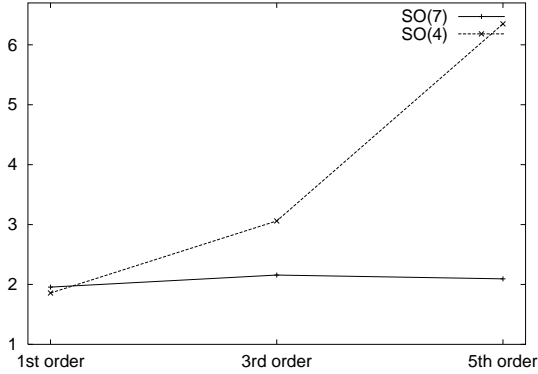


Figure 5. The ratio R/r of the extents obtained by the Gaussian expansion method for the IKKT model at orders 1,3 and 5. The two symbols correspond to the SO(4) Ansatz and the SO(7) Ansatz respectively. The result for the SO(4) Ansatz grows with the order.

der, and the results strengthened the conclusion of Ref. [10]. In Figs. 4 and 5 we show the free energy and the ratio R/r of the extents obtained up to the 5th order [11].

4.2.2. Monte Carlo simulation

Although the results of the Gaussian expansion method are encouraging and deserve further investigations, it is also important to confirm the results by Monte Carlo simulation from first principles. This approach will also allow us to understand the mechanism for the collapsing of the eigenvalue distribution of A_μ .

An important point to note here is that the fermion determinant $\det M = |\det M| e^{i\Gamma}$ is actually complex because the fermionic matrices Ψ_α transform as 10d Majorana-Weyl fermion, which is essentially chiral. (In Euclidean space chiral determinants are generally complex.) This poses the notorious technical problem known as the ‘complex-action problem’. As a first step, the phase-quenched model

$$Z_0 = \int dA e^{-S_b} |\det M| \quad (18)$$

has been simulated in Ref. [4]. We shall denote the VEV with respect to this partition function by $\langle \cdot \rangle_0$. The results for the order parameters $\langle \lambda_i \rangle_0$ are shown in Fig. 6. If one makes a linear extrapolation to $N = \infty$, one finds that all the $\langle \lambda_i \rangle_0$ converge to the same value, meaning that there is no SSB in the phase-quenched model. This implies that the phase of the fermion determinant plays a crucial role in the SSB if it happens at all (Refs. [5,8] support this scenario).

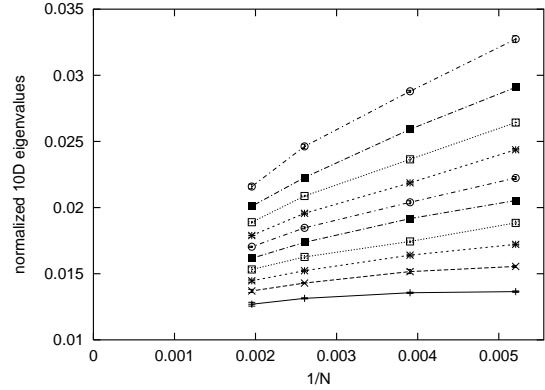


Figure 6. The 10 eigenvalues of the moment of inertia tensor in the *phase-quenched* model are plotted against $1/N$.

In order to study the effect of the phase, a new method has been considered [9]. Let us first normalize the eigenvalues of the moment of inertia tensor as

$$\tilde{\lambda}_i = \frac{\lambda_i}{\langle \lambda_i \rangle_0} . \quad (19)$$

Then we define the distribution

$$\rho_i(x) = \langle \delta(x - \tilde{\lambda}_i) \rangle , \quad (20)$$

which has the factorization property

$$\rho_i(x) = \frac{1}{C} \rho_i^{(0)}(x) w_i(x) , \quad (21)$$

where $\rho_i^{(0)}(x) = \langle \delta(x - \tilde{\lambda}_i) \rangle_0$ denotes the distribution defined in the phase-quenched model (18) and $C = \langle e^{i\Gamma} \rangle_0$ is a normalization constant.

The weight factor $w_i(x)$, which represents the effect of the phase, can be obtained by performing the constrained simulation

$$Z_i(x) = \int dA e^{-S_b} |\det M| \delta(x - \tilde{\lambda}_i) , \quad (22)$$

and calculating the expectation value of $e^{i\Gamma}$. This calculation is the most time-consuming part because of the oscillating phase, but one can still do it for moderate N . Various virtues of the method, as compared with the standard reweighting method, are discussed in Ref. [58].

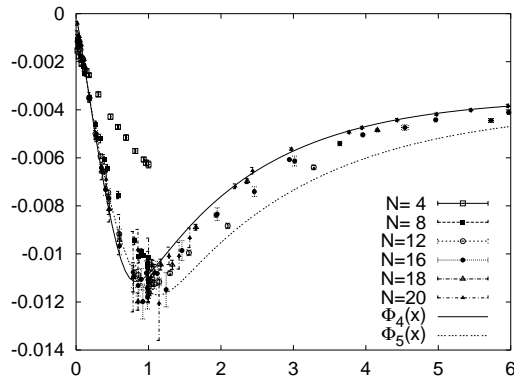


Figure 7. The function $\Phi_4(x) \equiv \frac{1}{N^2} \ln w_4(x)$ is plotted for various N . The solid curve represents a fit to some analytic function. The dotted curve represents a similar fit to the data for $\Phi_5(x)$.

The distribution $\rho_i^{(0)}(x)$ for the phase-quenched model is peaked at $x = 1$ due to the chosen normalization (19). The weight factor $w_i(x)$, on the other hand, turned out to have a minimum around $x \sim 1$ (see Fig. 7), and as a result the distribution $\rho_i(x)$ for the full model has a double-peak structure. Which of the two peaks becomes dominant at large N may depend on i . If it turns out that the peak at $x > 1$ dominates for $i \leq 4$, but the peak at $x < 1$ dominates for $i \geq 5$, we are able to obtain 4d space-time.

A crucial point in this approach is that

$$\Phi_i(x) \equiv \frac{1}{N^2} \ln w_i(x) \quad (23)$$

scales with N as one can see from Fig. 7. This scaling behavior is also understandable by general arguments [9]. Using the scaling function $\Phi_i(x)$ extracted in this way, one can estimate the height of the two peaks in the distribution $\rho_i(x)$ at much larger N . Preliminary results for $N = 64, 128$ [9] are encouraging, but it remains to be seen whether one can definitely conclude that 4d space-time appears in the IKKT model.

5. Lattice noncommutative geometry

In this Section we discuss noncommutative geometry, which has deep connections to string theory. In particular it was shown by Seiberg and Witten [59] that field theories in noncommutative geometry appear as a certain low-energy limit of string theory, and this triggered a tremendous boom in this subject. Among other things it was realized that such theories have various dynamical properties that ordinary field theories do not have. This is due to the UV/IR mixing effect, which was discovered in the one-loop calculation [60]. Calculations beyond one-loop become complicated because of this effect, and perturbative renormalizability is not proved even for simple scalar field theories [61]. This raises some suspicion that these theories are actually not well-defined nonperturbatively or the UV/IR mixing effect is merely a one-loop artifact.

Fortunately now we know how to regularize these theories on the lattice. In fact it was found that twisted reduced models at finite N can be interpreted as lattice-regularized field theories in noncommutative geometry [19]. This is a refinement of the earlier work [16], which pointed out the connection between twisted reduced models and noncommutative field theories.

Noncommutative geometry is characterized by the commutation relation among the space-time coordinates

$$[\hat{x}_\mu, \hat{x}_\nu] = i\theta_{\mu\nu} , \quad (24)$$

where \hat{x}_μ is a Hermitian operator. When we replace ordinary coordinates x_μ by the noncommut-

ing ones \hat{x}_μ , the field $\phi(x)$ should be replaced by $\hat{\Phi} = \phi(\hat{x})$, which is also an operator.

In fact this setting can be put on a periodic L^D lattice in such a way that there is a one-to-one correspondence between a field $\phi(x)$ on the lattice and a $N \times N$ matrix Φ . This means in particular that

$$L^D = N^2 \quad (25)$$

from the matching of the dynamical degrees of freedom. Using this matrix-field correspondence, one can derive the *noncommutative* lattice field theories from twisted reduced models [19]. Assuming the canonical form for the noncommutative tensor $\theta_{\mu\nu}$ in (24), its scale⁴ is found to be

$$\theta = \frac{1}{\pi} L a^2, \quad (26)$$

where a is the lattice spacing.

If one takes the planar limit sending N to infinity with fixed a , one obtains $\theta = \infty$. On the other hand, the twisted reduced model becomes equivalent to large N field theories in this limit as we discussed in Section 3.2. This is a non-perturbative account of the well-known fact that noncommutative theories at $\theta = \infty$ are equivalent to large N theories, which can be easily shown diagrammatically (see footnote 5).

In order to obtain noncommutative theories at finite θ , one has to take the large N limit and the continuum limit simultaneously. More specifically one has to take the limits $N \rightarrow \infty$ and $a \rightarrow 0$ in such a way that $N^{2/D} a^2$ is fixed. This corresponds to the double scaling limit we discussed in Section 2. In what follows we discuss the dynamics of specific theories, which have been studied by Monte Carlo simulation.

5.1. NC Yang-Mills theory on the lattice

As the simplest possible gauge theory in non-commutative geometry, 2d pure Yang-Mills theory has been studied by Monte Carlo simulation [21] using the twisted Eguchi-Kawai model (6). The planar limit of the theory is solved on the lattice by Gross and Witten [62], so we can refer to the result in our analysis. Let us consider the

⁴In the $D = 2$ case, for instance, θ is defined by $\theta_{\mu\nu} = \theta \epsilon_{\mu\nu}$.

VEV of the Wilson loop $\langle W(I \times I) \rangle$, which is complex in general unlike in ordinary gauge theory because the noncommutativity θ breaks parity.

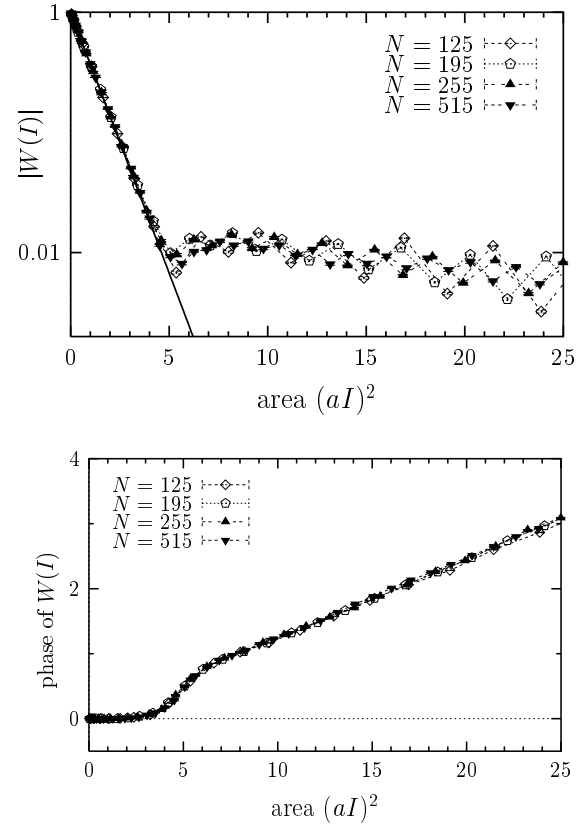


Figure 8. The polar coordinates of the complex Wilson loop $W(I)$ plotted against the physical area $A = a^2 I^2$. At small areas it follows the Gross-Witten area law (solid line). At larger areas the absolute value does not decay any more, but the phase increases linearly.

In Fig. 8 we plot the absolute value and the phase of the Wilson loop obtained for fixed $\theta = \frac{8}{\pi}$. One can see that the data in the small area regime $(aI)^2 \ll \theta$ agree with the Gross-Witten planar result. This is understandable because in the UV regime one cannot see the finiteness of θ , so the result becomes indistinguishable from that with $\theta = \infty$, namely the planar result. The coupling

constant β has been fine-tuned as a function of the lattice spacing a in such a way that the results in the planar regime scale. (In the present case we can use the Gross-Witten result to infer the tuning of the coupling constant.) The scaling in this regime is simply a consequence of the fact that the commutative large N gauge theory has a sensible continuum limit. What is highly nontrivial is that the scaling extends to larger area, where nonplanar diagrams start to contribute. This represents the continuum limit of the noncommutative theory with finite θ .

In particular we find that the phase of the Wilson loop grows linearly with the area as

$$(\text{phase}) = \theta^{-1} \times (\text{area}) , \quad (27)$$

which is reminiscent of the Aharonov-Bohm effect if we identify θ^{-1} with a static magnetic field traversing the 2d plane. Such an identification occurs commonly in noncommutative geometry, but the dynamical AB effect observed here awaits more profound understanding. Let us also comment that the IR behavior represented by (27) is clearly different from ordinary gauge theory. This confirms that the introduction of the noncommutativity θ can change the IR physics, which is not expected at the classical level. One should understand this fact as a consequence of the UV/IR mixing effect caused by the nonplanar diagrams.

5.2. NC ϕ^4 theory on the lattice

Let us discuss the effects of nonplanar diagrams more closely in the case of scalar field theories. For the one-loop correction to the inverse propagator, one obtains

$$F(p) = \int d^D q \frac{e^{i\theta_{\mu\nu} q_\nu p_\mu}}{q^2 + m^2} , \quad (28)$$

where the unusual phase factor $e^{i\theta_{\mu\nu} q_\nu p_\mu}$ is the only effect of the noncommutative geometry.⁵

Because of the ‘noncommutative phase’, the integration over the loop momentum q converges,

⁵ In the case of planar diagrams, this ‘noncommutative phase’ cancels. In the $\theta \rightarrow \infty$ limit, all the nonplanar diagrams vanish due to the oscillating phase, and only the planar diagrams survive. This is the diagrammatic account for the equivalence of the $\theta = \infty$ theory to the large N field theory.

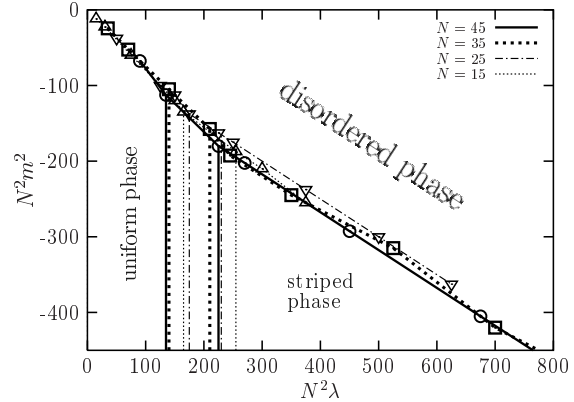


Figure 9. The phase diagram of the (2 + 1)d noncommutative ϕ^4 theory on the lattice.

and the function $F(p)$ becomes finite for $p \neq 0$. At $p = 0$ the phase vanishes, and the momentum integration has the usual UV divergence. This is reflected in the singularity of $F(p)$ at $p \sim 0$ as

$$F(p) \sim \frac{1}{|\theta p|^{D-2}} . \quad (29)$$

Thus the UV divergence of the commutative theory is transformed into the IR singularity with respect to the external momentum. This is the famous UV/IR mixing effect [60].

As a physical consequence of this effect, Gubser and Sondhi [63] conjectured the existence of the striped phase, where a nonzero momentum mode condenses, thus giving a position dependent VEV to the scalar field. This in particular means that the translational invariance is spontaneously broken. The analysis was based on self-consistent Hartree-Fock approximation at the one-loop, and it would be interesting to examine this conjecture by Monte Carlo simulation.

Let us consider (2+1)d NC ϕ^4 theory on the lattice [22], where two spatial directions are noncommutative as in Section 5.1, but now we also have a commuting (Euclidean) time direction in addition. The matrix model describing such a

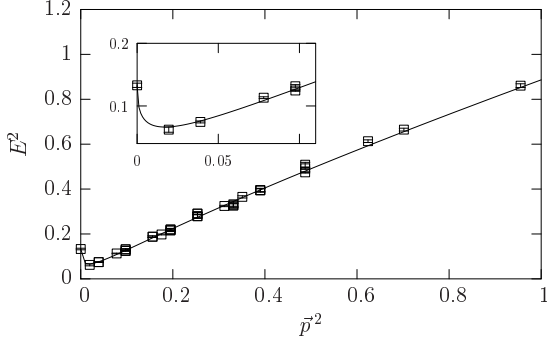


Figure 10. The dispersion relation in the disordered phase near the critical point.

theory is given by

$$\begin{aligned}
 S_{\text{NC}\phi^4} = & N \text{tr} \sum_{t=1}^T \left[\frac{1}{2} \sum_{\mu=1}^2 \{ \Gamma_{\mu} \Phi(t) \Gamma_{\mu}^{\dagger} - \Phi(t) \}^2 \right. \\
 & + \frac{1}{2} (\Phi(t+1) - \Phi(t))^2 \\
 & \left. + \frac{m^2}{2} \Phi(t)^2 + \frac{\lambda}{4} \Phi(t)^4 \right], \quad (30)
 \end{aligned}$$

where the shift operators Γ_{μ} in the noncommuting directions are defined by

$$\Gamma_{\mu} \Gamma_{\nu} = Z_{\mu\nu}^* \Gamma_{\nu} \Gamma_{\mu}, \quad (31)$$

$$Z_{\mu\nu} = e^{\pi i \frac{N+1}{N}} = Z_{\nu\mu}^*. \quad (32)$$

Fig. 9 shows the phase diagram obtained by Monte Carlo simulation. The disordered phase appears at large m^2 as in the well-known commutative case. Let us then decrease m^2 for a fixed coupling constant λ . When λ is small, the system undergoes the usual Ising-type phase transition into the uniformly ordered phase. However, when λ is sufficiently large, one obtains the striped phase as conjectured in Ref. [63]. Whether the width of the stripes becomes finite in the continuum limit is an interesting open question, which is currently being investigated.

This phenomenon can be understood more clearly by looking at the dispersion relation. Fig. 10 shows the dispersion relation obtained in the

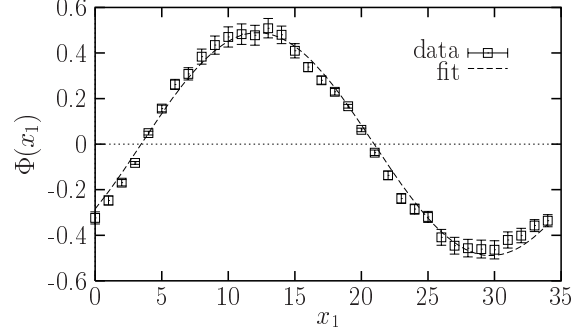


Figure 11. A snapshot of the configuration obtained just below the critical point with the same λ as in Fig. 10. The average has been taken over the x_2 direction, in which the value of the scalar field is uniform.

disordered phase near the critical point. One can see an anomalous behavior at $p \sim 0$, and as a result the minimum of the energy occurs at nonzero momentum. The data can be fitted to the form

$$E^2 = p^2 + M^2 + \frac{\lambda}{|\theta p|} \quad (33)$$

suggested by the one-loop calculation (29). Fig. 11 is a snapshot of the configuration obtained just below the critical point. The data can be nicely fitted to the sine function, in accord with the condensation of the nonzero momentum mode. If m^2 is even lower, the shape becomes more step-like.

6. Lattice supersymmetry via orbifolding

In this Section we comment on the recent proposal for a lattice construction of supersymmetric gauge theories based on reduced models [24]. Let us recall that the continuum version of reduced models can incorporate manifest SUSY even at finite N . Here the anti-commutator of Q and \bar{Q} yields a generator of the $U(1)^D$ transformation (9). Thus the translation is realized in the internal space, which is consistent with the identification of the eigenvalues of A_{μ} as the space-time coordinates described in Section 4.2.

The key to get a lattice theory from the con-

tinuum reduced model is the ‘orbifolding’, which is to impose a constraint on a matrix Φ such as

$$\Omega_j \Phi \Omega_j^\dagger = e^{ir_j} \Phi \quad \text{for } j = 1, \dots, d. \quad (34)$$

Solving the constraint explicitly, one obtains a d -dimensional lattice field theory. In particular the ‘charge vector’ r_j in (34) determines that the lattice field corresponding to the matrix Φ lives on the links connecting \vec{x} and $\vec{x} + \vec{r}$.

Part of the SUSY survives the orbifolding, which enables the restoration of the full SUSY in the continuum limit without fine-tuning. An extension to the noncommutative geometry is possible by making Ω_j in (34) noncommutative [64].

7. Summary

We have seen that the idea of Eguchi-Kawai reduction in large N gauge theories has developed in many different directions. Let us summarize them classifying large N reduced models into the lattice version and the continuum version.

In the lattice version there are a few ways to achieve the equivalence to large N gauge theories, and there are revived interests in this direction using the quenching or the partial reduction. On the other hand, the twisted reduced models have been given a new interpretation at *finite* N as a lattice regularization of noncommutative field theories. This motivated a different type of large N limit other than the planar limit, where non-planar diagrams also survive. Monte Carlo studies revealed intriguing dynamical properties of these theories caused by the UV/IR mixing.

The continuum version, on the other hand, has been obscure in the context of equivalence to large N gauge theories, but it suddenly became important as a nonperturbative formulation of superstring theory. We have discussed that the collapsing of the eigenvalue distribution, which was problematic in the context of Eguchi-Kawai equivalence, may provide the key to understand the dynamical generation of 4d space-time in 10d superstring theory. The ultimate goal in this direction is of course to derive the Standard Model from the IKKT model or from whatever matrix models describing nonperturbative superstrings.

REFERENCES

1. T. Eguchi and H. Kawai, Phys. Rev. Lett. **48** (1982) 1063.
2. N. Ishibashi, H. Kawai, Y. Kitazawa and A. Tsuchiya, Nucl. Phys. B **498** (1997) 467.
3. H. Aoki, S. Iso, H. Kawai, Y. Kitazawa and T. Tada, Prog. Theor. Phys. **99** (1998) 713.
4. J. Ambjørn, K. N. Anagnostopoulos, W. Bietenholz, T. Hotta and J. Nishimura, JHEP **0007** (2000) 011.
5. J. Nishimura and G. Vernizzi, JHEP **0004** (2000) 015; Phys. Rev. Lett. **85** (2000) 4664.
6. Z. Burda, B. Petersson and J. Tabaczek, Nucl. Phys. B **602** (2001) 399.
7. J. Ambjørn, K. N. Anagnostopoulos, W. Bietenholz, F. Hofheinz and J. Nishimura, Phys. Rev. D **65** (2002) 086001.
8. J. Nishimura, Phys. Rev. D **65** (2002) 105012.
9. K. N. Anagnostopoulos and J. Nishimura, Phys. Rev. D **66** (2002) 106008.
10. J. Nishimura and F. Sugino, JHEP **0205** (2002) 001.
11. H. Kawai, S. Kawamoto, T. Kuroki, T. Matsuo and S. Shinohara, Nucl. Phys. B **647** (2002) 153.
12. H. Kawai, S. Kawamoto, T. Kuroki and S. Shinohara, Prog. Theor. Phys. **109** (2003) 115.
13. G. Vernizzi and J. F. Wheeler, Phys. Rev. D **66** (2002) 085024.
14. T. Imai, Y. Kitazawa, Y. Takayama and D. Tomino, hep-th/0307007.
15. A. Connes, M. R. Douglas and A. Schwarz, JHEP **9802** (1998) 003.
16. H. Aoki, N. Ishibashi, S. Iso, H. Kawai, Y. Kitazawa and T. Tada, Nucl. Phys. B **565** (2000) 176.
17. A. Gonzalez-Arroyo and M. Okawa, Phys. Rev. D **27** (1983) 2397.
18. I. Bars and D. Minic, Phys. Rev. D **62** (2000) 105018.
19. J. Ambjørn, Y. M. Makeenko, J. Nishimura and R. J. Szabo, JHEP **9911** (1999) 029; Phys. Lett. B **480** (2000) 399; JHEP **0005** (2000) 023.
20. S. Profumo, JHEP **0210** (2002) 035.
21. W. Bietenholz, F. Hofheinz and J. Nishimura,

- JHEP **0209** (2002) 009.
22. W. Bietenholz, F. Hofheinz and J. Nishimura, Nucl. Phys. B (Proc. Suppl.) **119** (2003) 941; Fortsch. Phys. **51** (2003) 745; Acta Phys. Polonica B34 (2003) 4711; F. Hofheinz, Ph. D. Thesis, Humboldt Univ. Berlin, 2003; see also contribution by F. Hofheinz to these proceedings (hep-th/0309182).
 23. J. Ambjørn and S. Catterall, Phys. Lett. B **549** (2002) 253.
 24. A. G. Cohen, D. B. Kaplan, E. Katz and M. Unsal, JHEP **0308** (2003) 024; hep-lat/0307012; see also contribution by D.B. Kaplan to these proceedings (hep-lat/0309099).
 25. J. Kiskis, R. Narayanan and H. Neuberger, Phys. Rev. D **66** (2002) 025019.
 26. R. Narayanan and H. Neuberger, hep-lat/0303023.
 27. E. Brezin, C. Itzykson, G. Parisi and J. B. Zuber, Commun. Math. Phys. **59** (1978) 35.
 28. E. Brezin and V. A. Kazakov, Phys. Lett. B **236** (1990) 144.
 29. M. R. Douglas and S. H. Shenker, Nucl. Phys. B **335** (1990) 635.
 30. D. J. Gross and A. A. Migdal, Phys. Rev. Lett. **64** (1990) 127.
 31. G. Bhanot, U. M. Heller and H. Neuberger, Phys. Lett. B **113** (1982) 47.
 32. S. Profumo and E. Vicari, JHEP **0205** (2002) 014.
 33. D. J. Gross and Y. Kitazawa, Nucl. Phys. B **206** (1982) 440.
 34. H. Levine and H. Neuberger, Phys. Lett. B **119** (1982) 183.
 35. S. R. Das, Phys. Lett. B **132** (1983) 155.
 36. G. Parisi, Phys. Lett. B **112** (1982) 463.
 37. A. Gonzalez-Arroyo and M. Okawa, Nucl. Phys. B **247** (1984) 104.
 38. T. Eguchi and R. Nakayama, Phys. Lett. B **122** (1983) 59.
 39. F. R. Klinkhamer and P. van Baal, Nucl. Phys. B **237** (1984) 274.
 40. S. R. Das and J. B. Kogut, Phys. Lett. B **141** (1984) 105; Nucl. Phys. B **257** (1985) 141; Phys. Rev. D **31** (1985) 2704.
 41. S. R. Das, Rev. Mod. Phys. **59** (1987) 235.
 42. H. Neuberger, Phys. Lett. B **417** (1998) 141.
 43. Y. Kikukawa and H. Suzuki, JHEP **0209** (2002) 032.
 44. T. Inagaki, Y. Kikukawa and H. Suzuki, JHEP **0305** (2003) 042.
 45. W. Krauth and M. Staudacher, Phys. Lett. B **435** (1998) 350.
 46. W. Krauth, H. Nicolai and M. Staudacher, Phys. Lett. B **431** (1998) 31.
 47. P. Austing and J. F. Wheeler, JHEP **0102** (2001) 028; JHEP **0104** (2001) 019.
 48. P. Austing, G. Vernizzi and J. F. Wheeler, JHEP **0309** (2003) 023.
 49. T. Hotta, J. Nishimura and A. Tsuchiya, Nucl. Phys. B **545** (1999) 543.
 50. K. N. Anagnostopoulos, W. Bietenholz and J. Nishimura, Int. J. Mod. Phys. C **13** (2002) 555.
 51. J. Ambjørn, K. N. Anagnostopoulos, W. Bietenholz, T. Hotta and J. Nishimura, JHEP **0007** (2000) 013.
 52. A. Gonzalez-Arroyo and C. P. Korthals Altes, Phys. Lett. B **131** (1983) 396.
 53. M. Fukuma, H. Kawai, Y. Kitazawa and A. Tsuchiya, Nucl. Phys. B **510** (1998) 158.
 54. H. Aoki, S. Iso, H. Kawai, Y. Kitazawa, A. Tsuchiya and T. Tada, Prog. Theor. Phys. Suppl. **134** (1999) 47.
 55. P. Bialas, Z. Burda, B. Petersson and J. Tabaczek, Nucl. Phys. B **592** (2001) 391.
 56. K. N. Anagnostopoulos, J. Nishimura and P. Olesen, JHEP **0104** (2001) 024.
 57. J. Nishimura, T. Okubo and F. Sugino, JHEP **0210** (2002) 043.
 58. J. Ambjørn, K. N. Anagnostopoulos, J. Nishimura and J. J. Verbaarschot, JHEP **0210** (2002) 062.
 59. N. Seiberg and E. Witten, JHEP **9909** (1999) 032.
 60. S. Minwalla, M. Van Raamsdonk and N. Seiberg, JHEP **0002** (2000) 020.
 61. I. Chepelev and R. Roiban, JHEP **0005** (2000) 037.
 62. D. J. Gross and E. Witten, Phys. Rev. D **21** (1980) 446.
 63. S. S. Gubser and S. L. Sondhi, Nucl. Phys. B **605** (2001) 395.
 64. J. Nishimura, S. J. Rey and F. Sugino, JHEP **0302** (2003) 032.